

# Horizontal to Vertical Spectral Ratio seismic noise measurements to determine the location of bedrock beneath a saprolite soil in Ecuador

**Gabriela Torres**, Olegario Alonso-Pandavenes

*GEOTOP Equatorial Consulting. Quito. Ecuador. [geotop.equatorial@gmail.com](mailto:geotop.equatorial@gmail.com). Geology and Mining Engineering Faculty-FIGEMPA. Universidad Central del Ecuador. [omalonso@uce.edu.ec](mailto:omalonso@uce.edu.ec)*

Francisco Javier Torrijo Echarri

*Research Centre for Architecture, Heritage and Management for Sustainable Development (PEGASO), Department of Geotechnical Engineering, Universitat Politècnica de València, Camino de Vera s/n, 46022 Valencia, Spain; [fratorec@trr.upv.es](mailto:fratorec@trr.upv.es)*

**ABSTRACT:** A tailings dam in southeastern Ecuador was analyzed to determine the location of the rocky basement in the area where it was founded. By applying the passive seismic technique of Horizontal to Vertical Spectral Ratio (HVSR) at 25 station points and using the spectral analysis relationship of the horizontal and vertical components (H/V) of the seismic noise (fundamental ground frequency,  $f_0$ ), the soil parameters were defined by measuring the ambient seismic noise (microtremors). Selected seismic HVSR stations were correlated with geotechnical investigation boreholes used as control points, so the change in thickness and depth could be determined by comparing with the  $f_0$  obtained values. Data processing made it possible to define the H/V spectral relationship and obtain the ellipticity curve for each data set. The stratigraphic profile of the soil defined by the S-wave velocity was obtained to distinguish the soil materials and determine the depth of the rock. An empirical equation was established to determine the thickness of the sediments above the rocky substrate (a two-layer model), and it was applied to determine the soil thickness below each HVSR station. The applicability of the technique using the available information was analyzed using four interpretation profiles showing the depth at which the bedrock is located. These profiles were correlated with the geotechnical and weathered horizons (saprolite) of the subsoil observed in the boreholes' logs, making it possible to provide parameters for updating the existing stability models of the structure.

**KEYWORDS:** Saprolite soil; HVSR; H/V spectral ratio; bedrock depth; natural frequency of ground vibration;  $f_0$ .

## 1 INTRODUCTION

Tailings dams are important structures that contain waste materials (sterile or not) from a mine. The construction of these structures requires a deep knowledge of the foundation materials to preserve them during the life of the complex and further in time.

This research analyzes a tailings dam's foundation area in southeastern Ecuador, where the weathered igneous rock basement was transformed into a saprolite-type soil material due to tropical environmental and climate conditions.

The dam under study consists of a zoned structure dam composed of loose soil-like materials (granular and fine) and, at the beginning of its construction, was founded over igneous (intrusive) materials that were weathered and altered (saprolite), transitioning to a compact bedrock in depth.

The use of the Horizontal to Vertical Spectral Ratio (HVSR) technique, a passive seismic method based on the measurement of the natural vibration of the ground (using the surface waves or microtremors), has made it possible to determine the position and depth of the bedrock. That was possible by obtaining the fundamental frequency of ground vibration ( $f_0$ ) and the amplification or spectral ratio (H/V, also named amplification,  $A_0$ ). Using correlations with geological and geotechnical data from preliminary studies (control points of knowledge) through the determination of an empirical fitting curve (equation) and its validation, the thickness of sediment materials can be calculated at other points, so that the geological sections can be drawn.

The ease and quickness of this technique, together with the robustness of the measures, for determining the thickness of sediments on a compact basement, have been demonstrated. That permits extending the knowledge in a broad area, with a minimum of economic and survey data, and is valid in other zones.

## 2 LOCATION, GEOLOGY, AND PREVIOUS STUDIES

### 2.1 General Location and Geology

The study area is located in an actual mining area south of the Zamora-Chinchi province in southeastern Ecuador. It is approximately 40 km from the Peruvian border, in the Amazonian area, where the warm and rainy climate is classified as a tropical type.

In this area, the basement lithology is dominated by an igneous intrusive complex body known as the Zamora Batholith (Litherland et al., 1994). The igneous materials consist of a porphyritic intrusive body elongated in a NW-SE trend (200 by 50 km in size) and granodioritic to monzonitic composition.

In the same area, polymictic conglomerates (belonging to the Suárez Formation) also outcrop, overlain by sediments of the Hollín Formation, primarily interbedded sandstones and shales (Watson & Sinclair, 1927).

Over time, weathering and surface alteration by water filtration and the action of meteorological elements have developed a sandy clayey saprolite that is several meters thick and has varying degrees of alteration. These materials have not been mobilized (eluvial type).

### 2.2 Dam Foundation

The dam embankment rests on a tropical soil composed of a thick layer of saprolite (>30 m average), with a high degree of weathering of the native materials and not mobilized to the study area.

These materials were previously remediated and a part removed in the most altered layers before the dam construction processes to prevent settlement or a high degree of deformation in the structure (Torres, 2022).

### 2.3 Tailings Dam Structure

The granular material that comprises the embankment of the waste and tailings dam is made up of the following materials, as described in Torres (2022):

- Sapolite.  
This material was used to construct the dam's foundation, initial layers, and the inclined filter. Its primary function is to provide a layer of low-permeability material to reduce seepage in the lower part of the structure and through the dam section.
- Fine filter.  
It comprises of transitional materials between the sapolite and the coarse filter (next layer). It has a sand-type granulometry, consisting of clean river sands with a diameter of up to 19 mm and fine materials (content of less than 5%).
- Coarse filter.  
This filter is the transition between the fine filter and the outer rockfill. It corresponds to and is composed of gravel with a maximum size of 75 mm and a fines content of less than 15%.
- Selected rockfill.  
It has been used to form the foundation drains, in the basal drain layer, and to protect the outer face of the slope on the outer downstream face. It is composed primarily of sandstone rocks with a maximum diameter of 450 mm.
- Unclassified quarry material.  
Those materials form the outer face of the downstream slope and consist of sandstone-type materials obtained by blasting and classification processes before site placement.

All of these embankment materials, together with the sapolite that overlays the rocky basement, will be considered as sedimentary materials in terms of the further analysis that will be made.

### 2.4 Preliminary Studies

The preliminary studies conducted for the dam's construction were divided into four research campaigns over time. That includes: geotechnical testing, laboratory essays, control instrumentation, and monitoring.

The available data from research campaigns included: drilling with sample recovery, logs, and sample collections, borehole (in situ) and laboratory tests, geophysical surveys, and static cone penetration tests (CPT) (Torres, 2022). Some of the boreholes and surveys have not reached the rocky basement, so this investigation will complement this information to draw an accurate and better understanding of the foundation area.

These data allowed for adjusting the depth of the rocky basement and establishing correlation models used in this investigation.

## 3 METHODOLOGY

The research consisted of executing 25 HVSR test stations, each recording more than 20 minutes of ambient vibration (SESAME, 2003). The equipment used to perform the measures (Figure 1) was a three-geophone set-in-one element, oriented toward the magnetic north (corresponding with the north-south geophone component). The single element that contains the geophones was connected to a computer to set, control, and store the registered data.

The position and distribution of these measured points were not regularly located due to the dam's expansion works at the time of data collection, which have limited the application points' places, and they can be seen in Figure 2.



Figure 1. The geophysical equipment used in the investigation is shown to be placed in four locations. In the first row of pictures, it is set at the top and the middle of the embankment. In the second row, the left picture is on the west side (with a panoramic view of the embankment), and the right is at the bottom of the dam area.

This data collection was distributed along the body of the dam's levee and on the sides and base of the dam, where the geological and geotechnical information has a denser survey.

For orientation purposes, in Figure 2, the tailings and waste materials are deposited at the northwest blank area (where the north arrow is placed in the picture), and the bottom of the dam is in the southeast area of the picture.

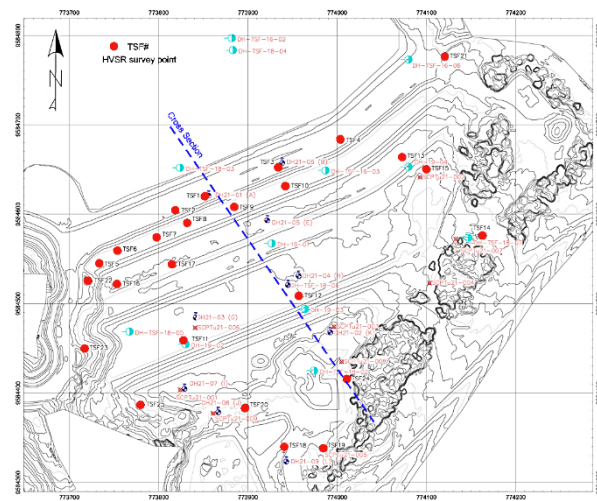


Figure 2. The location of the 25 measured HVSR points (red circles) and the reference investigations (blue circles) in the tailings dam area. Also, a cross-section point blue dashed line was indicated (modified from Torres, 2022).

Some HVSR measurement points were taken near or over previous direct survey points (boreholes or CPT tests and at less than 5 m radius) for further use as control points.

Geological and geotechnical information is available at those points, which will permit the establishment of a correlation between the sediment thickness (deposited over the rocky basement) and the results obtained from the HVSR processed measurements

### 3.1 Data Processing

The microtremor recordings obtained from the HVSR surveys were processed using the free software GEOPSY (Wathelet et

al., 2020) and following the guidelines established by the SESAME Project (SESAME, 2003; SESAME, 2004).

These ambient noise recordings were transformed into the frequency domain using a fast Fourier transform. This process was applied to the wavelets of each direction: N-S, E-W, and vertical (Z). After composing the two horizontal measured directions into one, the quotient of the horizontal spectra over the vertical one was calculated (H/V). That parameter is also known as amplification ( $A_o$ ).

This process yielded a dispersion curve from which the pairs of values ( $f_o$ ,  $A_o$ ) were extracted for each station point (see the examples in Figure 3).

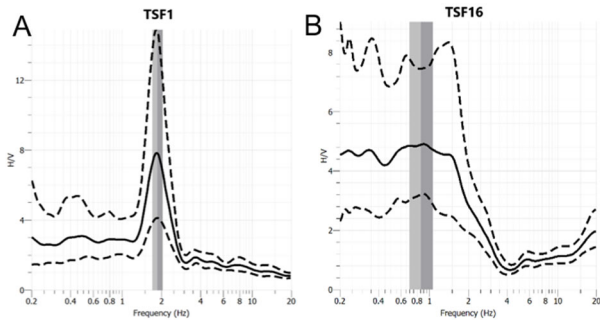


Figure 3. Two examples of processed dispersion curves (bold black continuous line). Figure A corresponds to the response of a typical curve exhibiting a clear peak (marked by grey bars) in the TSF-1 point, while Figure B represents a curve with what is named “a diffuse or broad peak” (TSF-16).

### 3.2 Correlation formula

Once the pairs of values have been obtained from the dispersion curves, a correlation formula needs to be established between the fundamental frequencies ( $f_o$ ) and the thicknesses of the sedimentary material deposited over the bedrock ( $H$ ).

That is proposed considering the work of Ibs-von Seth & Wohlenberg (1999), where they indicated that it is possible to establish an empirical relationship between the thickness of a sediment layer on a bedrock (a two-layer model concept) and the fundamental frequencies based on a potential relationship. The empirical correlation is expressed in Equation (1):

$$H = a f_o^{-b} \quad (1)$$

Where  $a$  and  $b$  are parameters that must be established from experimental values (for example, through an empirical curve fit),  $H$  is the thickness of non-compact or sedimentary materials deposited on a competent substrate (mostly rock, and expressed in m), and  $f_o$  would be the value of the fundamental frequency of the ground at the correlation point obtained from the HVSR measures (expressed in Hz).

Then, the proposed methodology consists in using the results obtained from the boreholes logs (where it was identified the sediment thickness and the saprolite transition zone) and the natural frequencies, obtained at the monitored HVSR points, a curve was fitted showing the relationship between this frequency ( $f_o$ ) and the thickness of the sediment and loose materials ( $H$ ), considered as a single element or layer.

This will allow us to calculate the thickness of the sediment beneath each HVSR station point and, thus, define the surface of the soil or sediment-rock interface, which can be drawn (Ibs-von Seth & Wohlenberg, 1999; Delgado et al., 2000; Alonso-Pandavenes et al., 2022).

## 4 RESULTS AND DISCUSSION

### 4.1 HVSR data processing. Results

After the field data campaign, the data were processed using the indicated software for each HVSR station point recorded. So, the  $f_o$ - $A_o$  value pairs were obtained as shown in Table 1.

In addition to the frequency and amplitude results for each HVSR sampled point, the same table shows the classification or analysis of the peak type that defines the ellipticity curve geometry obtained after the processing. Thus, it also indicates its characteristics (number of dominant peaks and their form).

In this study, a single and clear peak has predominated (see a type example in Figure 3A), which is synonymous with a high impedance contrast and a subhorizontal or low slope surface to horizontal interface (SESAME, 2004).

Table 1. Frequency and amplitude results for each HVSR sampled point also indicate the peak type obtained after the processing.

HVSR POINT	$f_o$ (Hz)	$A_o$ (dimensionless)	PEAK TYPE
TSF-1	1.85	8.61	single, clear peak
TSF-2	1.72	7.05	single, clear peak
TSF-3	1.71	5.43	single, clear peak
TSF-4	1.57	5.26	single, clear peak
TSF-5	2.31	3.74	broad, clear peak
TSF-6	1.98	3.65	serrate, clear peak
TSF-7	1.69	4.01	single, clear peak
TSF-8	1.79	6.05	single, clear peak
TSF-9	1.73	3.19	single, clear peak
TSF-10	1.71	6.20	broad, clear peak
TSF-11	1.92	3.92	single, clear peak
TSF-12	2.05	3.98	single, clear peak
TSF-13	1.74	3.09	single, clear peak
TSF-14	2.07	8.75	single, clear peak
TSF-15	2.31	3.09	diffuse peak
TSF-16	1.34	4.74	diffuse peak
TSF-17	1.83	6.82	single, clear peak
TSF-18	2.57	9.16	single, clear peak
TSF-19	2.26	7.90	single, clear peak
TSF-20	2.54	8.93	single, clear peak
TSF-21	2.13	4.24	broad, clear peak
TSF-22	1.38	32.96	double, clear peak
TSF-23	3.07	8.49	single, clear peak
TSF-24	1.94	8.14	single, clear peak
TSF-25	2.29	4.15	diffuse peak

### 4.2 Correlation Data and Empirical Equation Definition

To establish the empirical correlation that can define the  $a$  and  $b$  parameters of Equation (1), various results from direct surveys (primarily drilling) were used as control points.

Of the 25 HVSR test sites performed, nine measurements were selected that were applied on points previously investigated by drilling and for which information was available on the position of the rock substrate (not all drillings performed have reached this rocky material).

The nine station points and data used to perform the correlation between the natural frequency  $f_o$  and sedimentary

material thicknesses ( $H$ ) that overlay the rocky basement (considering natural and embankment materials as one set) are shown in Table 2 (where it is included the elevation of each HVSR measurement point in meters above sea level, m.a.s.l., as reference).

The data in Table 2 were represented graphically to perform the curve fit process. In this case, a potential fit was applied (see Figure 4). The value of fitting the obtained curve using the 9-point sample was 0.96 ( $R^2$ ), indicating a good correlation between the two parameters.

Table 2. Correlation between sediment thickness ( $H$ ) and the obtained natural frequencies ( $f_0$ ) at the nine control points

HVSR POINT	$f_0$ (Hz)	Elevation (m.a.s.l.)	Sediment thickness - $H$ (m)
TSF-1	1.85	1466.9	69
TSF-3	1.71	1467.2	75
TSF-9	1.73	1459.3	78
TSF-11	1.92	1441.0	60
TSF-12	2.05	1440.1	53
TSF-18	2.57	1416.0	35
TSF-20	2.54	1420.7	33
TSF-24	1.94	1420.9	53
TSF-25	2.29	1428.0	43

As can be observed in Figure 4, the control points exhibit a broad distribution of frequencies and sediment thickness. Those vary from 30 m to almost 80 m in the thickness value and from more than 1.50 Hz to up to 2.50 Hz in the frequency, ranging and being distributed regularly.

That is a reasonable control of the fitting method because the number of points used is low. However, even if a few data points were used, the results can be accurate depending on a broad dispersion of values (Alonso, 2024).

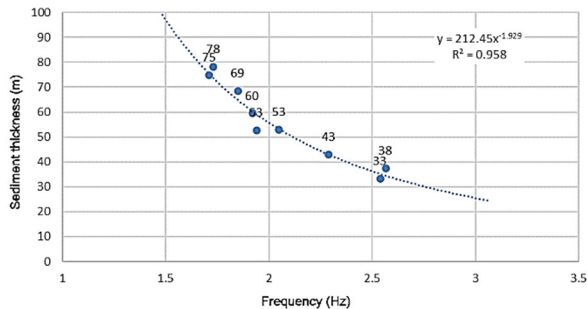


Figure 4. Potential trend line interpolation over the nine HVSR points selected as control points in Table 2.

The final fitting or correlation formula obtained was the following Equation (2):

$$H = 212.45 f_0^{-1.929} \quad (2)$$

This curve represents, for the study area, the relationship between the thicknesses ( $H$ ) of non-compact materials or sediments on a basement, considering the limitations indicated above, and the value of the fundamental vibration frequency obtained in an HVSR test.

Therefore, this empirical relationship defined by Equation (2) allows obtaining the thicknesses of the sediments below the position of other points tested in the area using the HVSR

surveys, and where there is no direct drilling or investigation for a direct correlation. Table 3 shows the calculated sediment thickness over the basement (in meters, third column) and the top of bedrock surface elevation for each HVSR surveyed point, considering the application elevation for each one using Equation (2).

In this way, a transverse profile to the dam embankment (a NW-SE direction cross-section) of the position of the rock basement was constructed and established, defining the geological cross-section at this position. It is shown in Figure 5 (the location of the section can be seen in Figure 2, marked as a blue dashed line).

Table 3. Calculated sediment thickness for every HVSR point, including surficial and bedrock elevations.

HVSR POINT	$f_0$ (Hz)	Surficial elevation (m.a.s.l.)	Calculated sediment thickness (m)	BEDROCK ELEVATION (m.a.s.l.)
TSF-1	1.85	1466.9	65	1402.1
TSF-2	1.72	1466.6	74	1392.2
TSF-3	1.71	1467.2	76	1391.7
TSF-4	1.57	1466.9	89	1378.0
TSF-5	2.31	1459.2	42	1417.0
TSF-6	1.98	1459.3	57	1402.2
TSF-7	1.69	1459.3	77	1382.3
TSF-8	1.79	1459.3	69	1390.3
TSF-9	1.73	1459.3	74	1385.5
TSF-10	1.71	1459.5	75	1384.1
TSF-11	1.92	1441.0	60	1380.6
TSF-12	2.05	1440.1	53	1386.9
TSF-13	1.74	1452.1	73	1379.3
TSF-14	2.07	1452.1	52	1399.8
TSF-15	2.31	1442.8	42	1400.5
TSF-16	1.34	1452.0	121	1331.2
TSF-17	1.83	1452.0	66	1385.6
TSF-18	2.57	1416.0	35	1381.5
TSF-19	2.26	1417.8	44	1373.8
TSF-20	2.54	1420.7	35	1385.5
TSF-21	2.13	1464.6	50	1415.1
TSF-22	1.38	1466.7	115	1352.1
TSF-23	3.07	1463.9	25	1439.4
TSF-24	1.94	1420.9	59	1361.7
TSF-25	2.29	1428.0	43	1385.0

In Figure 5, the boreholes' available data (indicated as colored hatched columns) and the results of the HVSR interpretation surveys (colorless columns) at each application elevation are also represented. In addition, the bedrock or basement materials are displayed as a crossed hatch. The lowest elevation of the bedrock is at 1355 m.a.s.l., with a low inclination of the bedrock surface towards the SE.

#### 4.3 Discussion

The natural frequency values ( $f_0$ ) obtained from field data processing range from 1.34 to 3.07 Hz, with an average value of  $1.98 \pm 0.4$  Hz. For these values, the peak amplification ( $A_0$ )

exceeds the minimum value of 2.00 recommended as a lower limit by the SESAME project (2004), and an average value of 6.82 has been obtained for this study, within a range from 3.09 to 32.96 (see values in Table 3).

The frequency interval obtained is broad enough to generate a range of frequency dispersion that can be correlated with the sediment thicknesses. They are varied and helpful in obtaining good results for the sedimentary basin analysis by applying the proposed methodology in this research, since it presents significant depth variations throughout the section investigated (Ibs-von Seth & Wohlenberg, 1999; Delgado et al., 2000; Alonso, 2024).

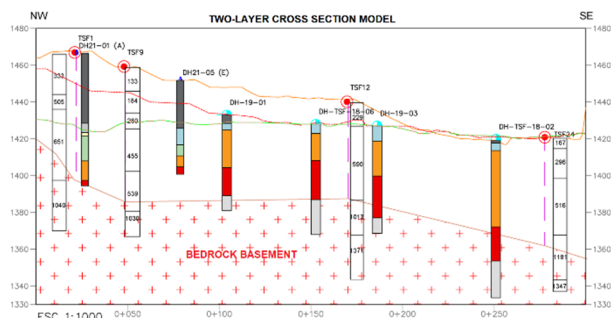


Figure 5. A transverse profile (see Figure 1 for location) of the dam area showing the basement surface (red-cross-hatch) distribution, which has its lowest elevation at 1355 m.a.s.l.

Most of the investigated points show clear and defined peaks as the maximum values, indicating that the fundamental frequency of the analyzed station has been determined in an area of high seismic impedance contrast. Furthermore, excluding the more diffuse points or serrated peaks, this definition of the frequency peaks indicates the presence of a natural substrate with a horizontal to subhorizontal surface or interface between soil, sediment, and rock, as the SESAME Project (2004) indicates.

The nine HVSR stations selected as control points for the ellipticity curve definition were eligible within a radius of less than 5 m from a direct investigation or borehole conducted during the various geotechnical exploration campaigns for maximum accuracy. With these data, and following a constrained model limitation criterion (Delgado et al., 2000; Alonso, 2024), a precise and accurate correlation was obtained with the sediment thickness values obtained from the boreholes conducted at each point. Also, as Nakamura (2000) indicates, the HVSR measures are a robust product with repetition capabilities (Mucciarelli and Gallipoli, 2001; Nakamura, 2019).

For reference purposes, borehole logs and the indications shown in their corresponding reports were used to correlate and compare boreholes' sediment thicknesses and the correlation with HVSR frequencies. That was because, in some boreholes, the recovered material did not allow for a precise characterization of the boundaries between the different materials, and high certainty and precision cannot be established in the borehole results with the materials drilled (Lunedei and Albarello, 2009).

The empirical curve fitting of thicknesses versus fundamental vibration frequencies was performed using nine control points. Despite the limited number of points, compared to other authors such as Ibs-von Seth & Wohlenberg (1999) or Hinzen et al. (2004) who used more than 30 control points, the fitting error is low ( $R^2 = 0.958$ ), resulting in a variation of around 5% in the definition of sediment thicknesses (or depths) concerning a frequency ( $f_0$ ) measured within the established range, as was analyzed in Alonso (2024).

The potential relationship established in Equation (2), between the thickness of sediments on a competent basement, presents an  $a$ -coefficient of 212.45, while in the  $b$ -coefficient, the value obtained has been -1.929. These values differ from those obtained in other investigations (such as in the Rhin River area by Ibs-von Seth & Wohlenberg, 1999), whose results for the same parameters are 146 and -1.375, respectively.

However, as Delgado et al. (2000) indicated, the  $a$ -factor would be related to the general geological characteristics of the area and the basin studied. That differs between both since the first work deals with alluvial Quaternary sediments, while this study was carried out on intrusive igneous materials with saprolite-type weathering horizons. Regarding the  $b$ -parameter, the same authors indicate that it would be related to the conditions and typology of the sediments, which, in this case, also differ from those tested elsewhere.

The value that varies the most is the term  $b$ . That may be due to the presence of the compacted materials used in the construction of the dam's embankment and the varying degrees of weathering of the saprolite and existing transition zones, since, in general, these are heterogeneous materials with varying texture and granulometry.

The work being carried out to raise the tailings dam's embankment has limited the use of a mesh or a regular arrangement of test points. A more regular arrangement or a mesh distribution parallel to the dam axis would likely have provided better results in fitting the curve to obtain the empirical relationship and estimate the depth to the basement using the same method.

## 5 SUMMARY AND CONCLUSIONS

The area where the mine tailings dam is located over a tropical saprolite soil has been investigated using the passive seismic HVSR technique (Nakamura, 1989).

The measured tests were carried out at 25 stations and completed using nine control points, distributed over the dam embankment and the tailings dam surroundings.

The obtained values in the HVSR processing have been correlated with the information by proximity to boreholes that have reached the basement. This has allowed us to reduce the degree of uncertainty in the models obtained and adjust them to the area's characteristics for reliable application in other studies with geological characteristics similar to those of the present study.

- For each HVSR test, the field data were processed, yielding the associated ellipticity curve. This defined the fundamental ground vibration frequency ( $f_0$ ) and its amplification or H/V spectral ratio ( $A_0$ ).
- The separation between the horizons at the sediment-rock contact was based on the considerations made by Nakamura (1989) and SESAME (2004), who indicated that  $V_s$  values greater than 600 m/s would correlate with a rocky substrate in a two-layer model. This differentiation was established in this study and was corroborated by the drilling logs.
- The results obtained for the thickness of the sediments or non-compact materials deposited above the bedrock and their relationship to the fundamental frequency,  $f_0$ , were graphically represented using the nine control points. The experimental Equation applicable to the remaining HVSR stations measured in the field was obtained by fitting a potential-type curve. This made it possible to define the bedrock position beneath all HVSR measuring stations easily. This also allowed us to verify the versatility of the technique and the reliability of the results obtained.

- The experimental curve obtained was applied to all HVSR seismic stations, defining the bedrock as located between 25 m and 42 m at the east and west abutments of the east dam. In the central section, the depth increases, reaching between 53 m and 77 m, measured from the elevation of the passive seismic points.
- By tracing a cross-section in the study area, it was possible to represent the position of the bedrock and compare it with existing information from previously conducted exploration campaigns, obtaining an irregular profile that represents the differential weathering of the rock.

This research presents a way to study an area by correlating of a simple, repeatable, robust, and inexpensive test with values obtained in a small number of direct tests (such as boreholes).

Furthermore, there is the possibility of expanding the results and obtaining a picture of the terrain (based on a simple two-layer model) solely through the application of HVSR tests.

On the other hand, the HVSR test allows depths of more than 100 m to be reached with field records lasting more than 30 minutes, allowing the investigation of tropical saprolite zones where the development of igneous rock alteration is significant.

Future research aims to establish more precise correlations through the inversion of the dispersion curve, based on restricted models. This way, the data obtained would correlate with shear wave velocity values in simple models with more than two layers. These shear wave velocity values are related to geotechnical parameters that can be demonstrated through this robust and straightforward test type.

## 6 REFERENCES

- Alonso Pandavenes, O. (2024) *Técnicas de sismica pasiva HVSR aplicadas a la geotecnia. Aplicación al estudio de Movimientos en Masa en la Planificación Territorial e Infraestructura Civil en Ecuador*. Ph.D. Thesis. Universitat Politècnica de València. Escuela Técnica Superior de Ingenieros de Caminos, Canales y Puertos. Available at: <http://hdl.handle.net/10251/202657>.
- Alonso-Pandavenes, O. et al. (2022) 'Basement tectonic structure and sediment thickness of a valley defined using HVSR geophysical investigation, Azuela valley, Ecuador', *Bulletin of Engineering Geology and the Environment*, 81(5), p. 210. Available at: <https://doi.org/10.1007/s10064-022-02679-y>.
- Delgado, J. et al. (2000) 'Microtremors as a Geophysical Exploration Tool: Applications and Limitations', *Pure and Applied Geophysics*, 157(9), pp. 1445–1462. Available at: <https://doi.org/10.1007/PL00001128>.
- Hinzen, K.-G., Weber, B. and Scherbaum, F. (2004) 'On the resolution of H/V measurements to determine sediment thickness, a case study across a normal fault in the Lower Rhine Embayment, Germany', *Journal of Earthquake Engineering*, 8(6), pp. 909–926. Available at: <https://doi.org/10.1080/13632460409350514>.
- Ibs-von Seht, M. and Wohlenberg, J. (1999) 'Microtremor measurements used to map thickness of soft sediments', *Bulletin of the Seismological Society of America*, 89(1), pp. 250–259. Available at: <https://doi.org/10.1785/BSSA0890010250>.
- Litherland, M., Aspden, J.A. and Jemielita, R. (1994) *Los cinturones metamórficos del Ecuador*.
- Lunedei, E. and Albarello, D. (2009) 'On the seismic noise wavefield in a weakly dissipative layered Earth', *Geophysical Journal International*, 177(3), pp. 1001–1014. Available at: <https://doi.org/10.1111/j.1365-246X.2008.04062.x>.
- Mucciarelli, M. and Gallipoli, M.R. (2001) 'A critical review of 10 years of microtremor HVSR technique', *Bollettino di Geofisica Teorica ed Applicata*. Available at: <https://www.scopus.com/inward/record.uri?eid=2-s2.0-0348094973&partnerID=40&md5=4df1c128767bb1a2cb45d3766377597c>.
- Nakamura, Y. (1989) 'A method for dynamic characteristics estimation of subsurface using microtremor on the ground surface', *Quarterly Report of Railway Technical Research*, 30, pp. 25–33.
- Nakamura, Y. (2000) 'Clear Identification of Fundamental Idea of Nakamura's Technique and Its Applications', *The 12th World Conference on Earthquake Engineering* [Preprint].
- Nakamura, Y. (2019) 'What Is the Nakamura Method?', *Seismological Research Letters*, 90, pp. 1437–1443. Available at: <https://doi.org/10.1785/0220180376>.
- SESAME Project (2003) *Measurement Guidelines*. Deliverable D08.02 WP02. Grenoble: European Commission, p. 96. Available at: [https://web.archive.org/web/20160428020935/http://sesame.geopsy.org/Delivrables/D08-02\\_Texte.pdf](https://web.archive.org/web/20160428020935/http://sesame.geopsy.org/Delivrables/D08-02_Texte.pdf) (Accessed: 15 June 2021).
- SESAME Project (2004) *Guidelines for the implementation of the H/V spectral ratio technique on ambient vibrations measurements, processing and interpretation*. Deliverable D23.12 WP12. Grenoble: European Commission, p. 62. Available at: [http://sesame.geopsy.org/Papers/HV\\_User\\_Guidelines.pdf](http://sesame.geopsy.org/Papers/HV_User_Guidelines.pdf) (Accessed: 15 June 2021).
- Torres, G. (2022) *Aplicación de Medidas del Ruido Sísmico Ambiental para definir la posición del Basamento Rocoso en una Presa de Relaves*. Master Thesis. UNED - CEDEX.
- Wathelet, M. et al. (2020) 'Geopsy: A User-Friendly Open-Source Tool Set for Ambient Vibration Processing', *Seismological Research Letters*, 91(3), pp. 1878–1889. Available at: <https://doi.org/10.1785/0220190360>.
- Watson, T. and Sinclair, J. (1927) 'Geological Explorations East of the Andes in Ecuador', *AAPG Bulletin*, pp. 1263–1266.